



PII S0016-7037(01)00756-6

Water in martian magmas: Clues from light lithophile elements in shergottite and nakhlite pyroxenes

R. C. F. LENTZ,*¹ H. Y. MCSWEEN JR.,¹ J. RYAN,² and L. R. RICIPUTI³¹Department of Geological Sciences, University of Tennessee, Knoxville, TN 37996-1410, USA²Department of Geology, University of South Florida, Tampa, FL 33620, USA³Chemical and Analytical Sciences Division, Oak Ridge National Laboratory, Oak Ridge, TN 37831, USA

(Received September 18, 2000; accepted in revised form July 10, 2001)

Abstract—There is abundant geomorphic evidence that Mars once had potentially significant amounts of water on its surface. Bulk martian meteorites are curiously dry, and hydrated minerals found in some of these rocks are also surprisingly low in water content. We look for evidence of pre-eruptive magmatic water by analyzing the abundances of Li, Be, and B, light lithophile elements that have proven useful in tracking water–magma interactions in terrestrial studies because of their solubility differences. We performed secondary ionization mass spectrometer (SIMS) analysis of these incompatible elements in pyroxenes of two nakhlites and two basaltic shergottites, with quite different results. In Nakhla and Lafayette, all three elements behave as incompatible elements, with increasing abundance with magma evolution from pyroxene cores to rims. In Shergotty and Zagami, Be increases, but both B and Li decrease from pyroxene cores to rims. From terrestrial studies, it is known that Be is virtually insoluble in aqueous hydrothermal fluids, whereas B and Li are quite soluble. We suggest, therefore, that the elemental decreases in the shergottite pyroxenes reflect dissolution and loss of B and Li in a hot, aqueous fluid exsolved from the magma.

Consistent with our results, recent experimental work proposes that the shergottite parent magmas contained 1.8 wt% water (Dann et al., 2001). We suggest that the pyroxene cores grew at depth (>4 km) where the water would remain dissolved in the magma. Once the magma began to ascend, the volatile component could gradually exsolve, removing the soluble species from the melt in the process. Upon eruption, the volatile component might then be lost through degassing, leaving a B- and Li-depleted magma to crystallize pyroxene rims and plagioclase. This magmatic water might have derived from the martian mantle or resulted from deep crustal contamination. If the water contents proposed for the shergottite magmas, and implied by our results, are typical of basaltic magmas on Mars, this mechanism could provide an efficient method of delivering substantial amounts of water to the martian surface at later times in martian history. Copyright © 2001 Elsevier Science Ltd

1. INTRODUCTION

The volatile inventory and outgassing history of Mars are controversial issues. With recent discussions of possible oceans in middle Mars history (Head et al., 1999, and references therein), modern near-surface aquifers (Malin and Edgett, 2000), and putative life on Mars (McKay et al., 1996), it has become particularly important to establish various details concerning this water: how much was on the surface of Mars, when in martian history, for what duration, and from what source. Numerous estimates have been made of past martian water volumes on the basis of surface feature morphologies (flood channels, outwash plains, erosional features), relative atmospheric gas abundances, and volumetric estimates of volcanic material with assumed magma water contents (summarized by McSween and Harvey, 1993). These methods yield water abundance estimates that span a huge range, from globally uniform layers 10 m to more than 400 m deep.

Assuming most surface water was generated through outgassing during volcanic activity, several authors have focused on determining the water contents of the igneous martian meteorites. However, the measured bulk meteorite water contents from high temperature fractions (i.e., magmatic) are quite low,

generally on the order of 130 to 350 ppm (Karlsson et al., 1992). These abundances seem too low for such rocks to be the source for all the water that once flowed on the martian surface. It should be noted, though, that the water content of a volcanic rock does not necessarily reflect the pre-eruptive magma water content. Many terrestrial rocks with measured low water contents have other compositional evidence, such as magmatic inclusions, which point to water-rich parent magmas (Sisson and Grove, 1993; Sisson and Layne, 1993). Several martian meteorites do contain trapped magmatic inclusions containing daughter minerals typically considered hydrous (kaersutite, biotite, apatite) but the implications of their presence are unclear. Originally, the identification of these minerals prompted suggestions of significant magma water contents at depth (Floran et al., 1978; Johnson et al., 1991; McSween and Harvey, 1993). However, measured H contents of these “hydrous” phases imply lower than expected water contents (Watson et al., 1994), and laboratory experiments have since suggested that the kaersutite compositions can be grown under rather dry conditions (e.g., Popp et al., 1995). On the other hand, King et al. (1999) suggested that these kaersutitic amphiboles may have experienced oxidation and dehydrogenation and thus may not have crystallized under low water activity conditions. Studies of Zagami demonstrate that even if these early-crystallized amphiboles did imply the presence of water, late-stage melt pock-

* Author to whom correspondence should be addressed (rlentz@utk.edu).

Table 1. Partition coefficients for trace elements.^a

Element	D cpx/melt	D plag/melt	D fluid/melt (solubility)	
			Range	
Li	0.20	0.23	0.80	2.27
Be	0.011	0.27	0.01	0.01
B	0.016	0.05	1.14	2.08
Ti	0.4	0.04		
Y	0.9	0.03		
Ce	0.15	0.12		
V	1.35			
Zr	0.1	0.048		
Sr	0.06	1.83		

^a Pyx/melt coefficients for Li, Be, and B from Brenan et al. (1998a); plag/melt for Li, Be, and B from Ryan (1989). Fluid/melt coefficients for Li, Be, B are calculated from cpx/fluid coefficients in Brenan et al. (1998b). Range due to variable D (fluid/melt) for Al/Si range in shergottite pyroxenes. All other trace element coefficients are from Rollinson (1993).

ets suggest late conditions were quite dry (McCoy et al., 1999). Given these conflicting interpretations, we conclude that the hydrous minerals do not provide an unambiguous, and thus reliable, constraint on water in martian meteorite parent magmas.

For this study, we examine the geochemical behaviors of the light lithophile elements during magma evolution. Lithium, beryllium, and boron have proven useful in terrestrial studies of the role of water in subduction zone magmas (e.g., Noll et al., 1996). Their usefulness is due to their different solubilities in hydrothermal fluids: Be is virtually insoluble in H₂O-rich fluids (Measures and Edmond, 1983; Ryan and Langmuir, 1988; Brenan et al., 1998b; Ryan, 2000), B is highly soluble in fluids ~200°C (Seyfried et al., 1984; Ryan and Langmuir, 1993), and Li is highly soluble in fluids >375°C, showing particularly strong mobility under high-grade metamorphic conditions (Seyfried et al., 1984; Ryan and Langmuir, 1987; Brenan et al., 1998b). In the absence of a hot aqueous fluid, all three elements behave incompatibly (Table 1), and thus track magma evolution during mineral growth.

We decided to focus on two basaltic shergottites (Shergotty and Zagami) and two nakhlites (Nakhla and Lafayette), with the notion of comparing results from the two distinct crystallization histories of the lithologies (Fig. 1). These four meteorites also share the advantage of being falls and have therefore experienced less terrestrial weathering and contamination than Antarctic or Saharan martian meteorites. More important, the meteorites are each characterized by zoned clinopyroxene with cores and rims interpreted as representing different periods of mineral growth during crystallization, giving us geochemical views into two periods of magma evolution.

Despite the fact that martian meteorites are among the most comprehensively studied geologic samples, the systematics of the light lithophile elements in these meteorites are virtually unknown. Bulk rock samples have not been analyzed, particularly for B and Be, because current techniques require the destruction of too much material. There are a few bulk Li values in the literature (compiled by Meyer, 1998), but Li, Be, and B in minerals have only been measured via secondary

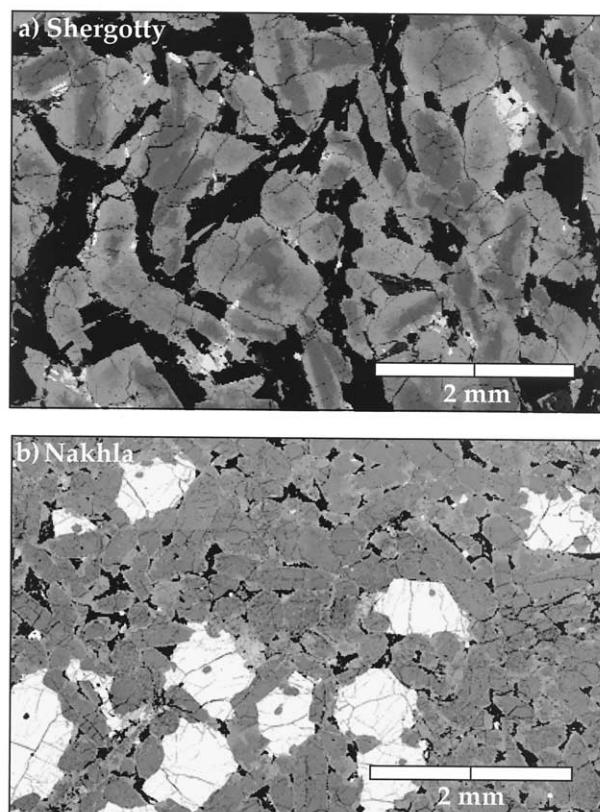


Fig. 1. Images illustrating the textures of the two meteorite types used in this study. (a) Fe distribution map of Shergotty showing Mg-rich pyroxene cores (dark gray) with surrounding Fe-rich rims (light gray) and interstitial plagioclase, now shocked to feldspathic glass (black). (b) Backscatter electron image of Nakhla with similar augite zonation, but significantly thinner rims. Plagioclase is restricted to small mesostasis pockets (black). White grains are Fe-rich olivine.

ionization mass spectrometer (SIMS) by Chaussidon and Robert (1999). Their focus was primarily on the isotopic ratios of Li and B, and their abstract did not report abundances, except to note that in the basaltic shergottites, B concentrations in maskelynite are 5 to 10 times lower than in pyroxene. Here, we examine the ramifications of the relative abundances of Li, Be, and B, determined by SIMS, in early and late crystallizing minerals in basaltic shergottites and nakhlites.

2. SAMPLES AND METHODS

Shergotty and Zagami are characterized by strongly zoned pyroxenes (augite and pigeonite) and interstitial plagioclase (now shocked to feldspathic glass; Fig. 1a). The meteorites' bulk compositions and crystallization histories are so similar that they are thought to be closely related magmatically (e.g., Stolper and McSween, 1979; Wadhwa et al., 1994). Only in grain size are they significantly different, which has been attributed to a faster cooling rate for Zagami (McCoy et al., 1992). Several studies have concluded from experiments and petrographic relationships that, most likely, there were two stages of growth: the Mg-rich pyroxene cores grew at depth, and the Fe-rich rims crystallized later, with plagioclase, after a change in crystallization conditions associated with shallow intrusion or extrusion (e.g., Stolper and McSween, 1979; McCoy et al., 1992; Lentz and McSween, 2000).

Nakhla and Lafayette are dominated by zoned augite and olivine, with plagioclase limited to fine sprays in mesostases pockets (Fig. 1b).

These petrographic relationships have been interpreted to reflect an extended period of augite crystallization, with plagioclase growth commencing only during the very latest stages of crystallization in isolated melt pockets (e.g., Harvey and McSween, 1992; Friedman Lentz et al., 1999). During this latest period, thin Fe-rich rims were added to the pyroxene grains.

One thin section each of Shergotty (USNM 321-2), Zagami (UNM 1019), Nakhla (USNM 426-4) and Lafayette (USNM 1505-2) was used for this study. For each section, five to seven pyroxene grains were analyzed, core and rim, with at least one five-point traverse measured per thin section. In addition, five to seven plagioclase grains (or feldspathic glass in the shergottites) were measured.

Trace element compositions were analyzed with a Cameca ims-4f ion probe at the Oak Ridge National Laboratory. Before gold-coating for SIMS analysis, each thin section was soaked for 2 h in a 1% mannitol solution and rinsed in B-free distilled water to combat surface B contamination (a method developed by R. Hervig; R. Hervig, personal communication), after which the section was promptly coated. Nakhla, Lafayette, and Shergotty were analyzed sequentially in a continuous session, whereas Zagami was analyzed several months later. The samples were bombarded with a 12.5 kV primary beam of $^{16}\text{O}^-$ ions at 10 nA and with a beam size of ~ 15 to $20\ \mu\text{m}$ for most pyroxene analyses. In cases where greater spatial resolution was necessary (to distinguish Zagami rims and to measure the narrow nakhlite plagioclase laths), the beam was reduced to 5 to $10\ \mu\text{m}$ with the current lowered to 1.5 to 3 nA; the number of measurement cycles was increased to compensate for lower counts. Nakhlite pyroxene rims proved to be thinner and more difficult to measure than had been anticipated. Thus, the actual "rim" measurements likely represent an average rim and core composition acquired by using a beam that was larger than optimal and that may have penetrated into underlying, less zoned pyroxene material (see Results).

Positive secondary ions were extracted by the secondary mass spectrometer with a mass resolution of ~ 600 and counted by using an electron multiplier. Energy filtering was used to avoid secondary ion interference (e.g., ^9Be and Al^{3+}). Two sets of elements were measured at each spot (Al, ^{30}Si , Ti, V, ^{86}Sr , Y, Zr, Ce and Na, K, Li, Be, B), with the measurement time of the first set acting as sputtering time before measuring B, in particular.

Calibration curves were derived by using multiple measurements of standards of natural minerals (Plag B, SanCarlos Olivine, Unknown Cpx, Wilberforce Augite, and W_A Diop) and glasses (NBS 610, 612, and 688, W2, QLO, BHVO, AGV, STM1, BIR, RGM, JDF-2, LUM37). Calibration data fell in linear trends and were fit with both linear and power law curves, giving correlation coefficients of $R^2 = 0.97$ to 1.0. Power law fits were ultimately chosen for the calibrations of Li, Be, and B because they supplied better matches for the low element abundances we expected for our samples. Detection limits were determined using the calibration equations by calculating the concentration of each element given a worst-case background rate of ~ 0.1 counts per second. These limits are all well below measured values (at least two orders of magnitude). Measurement precisions ($\sqrt{\text{no. of counts}}/\text{no. of counts}$) are mostly less than 4% relative, with the exceptions of Zr ($\sim 7\%$), Ce (up to $\sim 15\%$), and Be ($\sim 10\%$). The useful ion yields of Li relative to Si averaged 14.7 ± 3.2 , with only a plagioclase standard producing a large outlier at nearly twice the yield of the glasses, likely due to matrix effects. Pyroxene standards, however, fell nicely within the range of the glass standards. Be ion yields also showed minor variation with an average of 10.7 ± 3.9 , which are reportedly similar to those determined for a compilation of three different SIMS labs (R. Hervig, personal communication). However, B ion yields did have more variability, averaging 5.2 ± 2.6 , but showed no correlation between yield and standard concentration, suggesting we successfully removed any potential B contamination.

Major element compositions were determined, at approximately the same locations as the SIMS spots, with a Cameca SX-50 electron microprobe at the University of Tennessee. An acceleration voltage of 15 keV was used with a beam current of 20 nA, beam size of $1\ \mu\text{m}$, and 30-s count times. Well-characterized minerals were used as standards, and all analyses were corrected by using a company-supplied ZAF routine (P). These results were primarily used to determine pyroxene type (WoEnFs) and Mg# (Fig. 2).

Because plagioclase was a late crystallizing phase in both meteorite

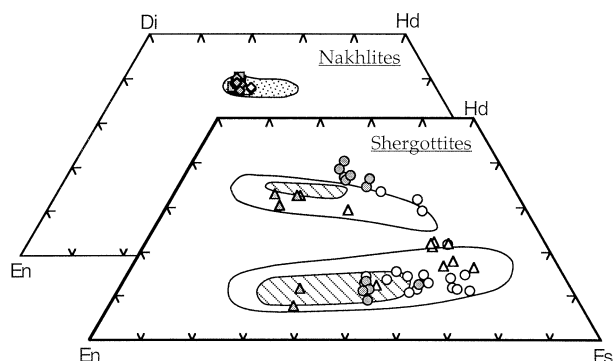


Fig. 2. Pyroxene quadrilateral showing major element compositions of cores (solid symbols) and rims (open symbols) for Nakhla (squares), Lafayette (diamonds), Shergotty (triangles), and Zagami (circles) analyzed by SIMS in this study. Fields show typical compositions in the literature: stippled area for augite in nakhlites (Friedman Lentz et al., 1999), hatched area for "Normal Zagami" (McCoy et al., 1999), and open area for Shergotty (Hale et al., 1999). Note that our nakhlite augite rim compositions are not as Fe rich as seen in other studies, and the shergottite cores do not reach the Mg-rich extremes.

lithologies, abundances of the light lithophile elements in plagioclase reveal little about the main stages of magma evolution. In addition, there is the complication of whether the shock process that converted shergottite plagioclase to feldspathic glass affected the light lithophile elements (Chaussidon and Robert, 1999). However, the relative values are certainly reliable, so for now the plagioclase data have only been applied to evaluate the quality of the Be pyroxene data.

3. RESULTS

Trace element data are presented in Tables 2 and 3, and Figure 3 illustrates element behavior in the pyroxenes. Trace elements are plotted vs. TiO_2 rather than Mg# for consistency because the Ti data were acquired by using the SIMS at the same time as other trace element data.

For the most part, the nakhlite data exhibit incompatible element enrichment trends when plotted against TiO_2 , although V shows more scatter than do the other elements. Strontium behaves incompatibly throughout because of the late crystallization of plagioclase. Note, however, that the "rim" compositions (open symbols) are quite mixed with the "core" measurements (solid symbols) in many cases. Our data do not seem to show the full extent of magma evolution previously detected by pyroxene zoning in these two meteorites, especially Nakhla (Harvey and McSween, 1992; Friedman Lentz et al., 1999). This is also apparent in major element data (Fig. 2), where the rims plot essentially identically to the cores. This is likely due to the difficulty in analyzing the thin rims and suggests that what we here labeled "rim" represents a core/rim mix and not the fully evolved magma we had hoped to measure (see Methods).

The shergottite data show much more scatter than the nakhlite data, especially in the rim compositions, but there are discernible trends that are consistent between Shergotty and Zagami. In both meteorites, Y, Zr, and Sr abundances correlate with increasing TiO_2 , consistent with their incompatibility in pyroxenes (Table 1), and there are no detectable differences between augite and pigeonite trace element abundances. Only two of these trace elements stand out with different behaviors

Table 2. SIMS trace element data for augites (unless otherwise noted) in nakhlites.

Specimen and Site	TiO ₂ (wt%)	V (ppm)	Sr (ppm)	Y (ppm)	Zr (ppm)	Ce (ppm)	Li (ppm)	Be (ppm)	B (ppm)	Be (ppm) in plagioclase	
Nakhla											
px 3	Core	0.364	210	37.8	5.3	4.7	4.8	4.77	0.0009	0.47	0.31
	Rim	0.258	177	29.0	4.3	4.8	4.3	5.99	0.0033	2.02	0.38
px 4	Core	0.262	193	29.6	4.2	3.3	4.3	4.94	0.0005	0.50	0.48
	Midpoint	0.265	193	26.9	4.3	3.3	4.3	5.59	0.0006	0.45	0.42
	Rim ^a	0.359	224	40.9	6.4	5.5	6.8	3.76	0.0265	0.70	0.55
	Midpoint	0.314	193	31.2	5.2	4.0	4.6	5.48	0.0006	0.51	0.59
	Rim	0.288	189	31.6	4.8	3.6	4.5	5.55	0.0007	0.47	0.55
px 5	Core	0.344	191	36.9	5.1	3.9	4.7	5.40	0.0010	0.46	
	Rim	0.308	176	32.8	4.9	3.6	4.6	5.52	0.0007	0.44	
px 6	Core	0.383	212	39.2	5.7	5.0	5.1	3.86	0.0057	0.50	
	Rim	0.418	193	44.7	6.6	5.1	5.5	5.34	0.0023	0.54	
px 7	Core	0.320	216	31.2	5.1	3.9	4.7	5.46	0.0007	0.51	
	Rim	0.452	198	46.4	7.5	5.8	5.9	4.64	0.0019	0.66	
px 8	Core	0.309	174	30.3	4.8	3.6	4.5	4.60	0.0013	0.77	
	Rim	0.390	213	37.0	5.8	4.1	4.7	3.85	0.0008	0.68	
px 8	Core	0.288	168	28.5	4.5	3.3	4.4	4.89	0.0009	0.81	
	Rim										
Lafayette											
px 1	Core	0.469	217	43	7.7	6.4	5.9	5.67	0.0025	0.93	0.74
	Midpoint	0.457	197	47	7.2	6.0	6.0	6.20	0.0015	0.81	0.72
	Rim ^a	0.345	190	42	7.4	12.9	5.4	4.51	0.067	1.90	0.26
	Midpoint	0.271	165	29	4.6	3.7	4.4	5.85	0.0021	0.83	0.45
	Rim	0.264	161	31	4.2	3.4	4.3	6.69	0.0019	1.02	0.39
px 3	Core	0.373	184	43	5.7	5.2	5.2	5.42	0.0024	1.02	0.74
	Rim	0.273	170	32	4.4	4.0	4.2	6.44	0.0062	0.90	0.54
px 5	Core	0.439	193	53	7.1	5.5	5.5	6.06	0.0013	0.97	
	Rim	0.301	184	33	4.9	4.2	4.6	5.38	0.0071	2.01	
px 6	Core	0.328	177	36	5.1	4.3	4.8	5.59	0.0009	0.92	
	Rim	0.304	180	29	4.6	4.0	4.5	5.95	0.0015	0.98	
px 7	Core	0.446	190	46	7.9	6.3	5.7	5.39	0.0019	0.93	
	Midpoint	0.263	158	29	4.8	3.7	4.3	6.21	0.0011	0.87	
	Rim	0.277	167	40	4.4	3.8	4.5	6.51	0.0020	1.14	
	Midpoint	0.306	168	35	5.1	4.2	4.6	5.88	0.0013	0.89	
	Rim	0.303	163	37	5.3	5.2	5.0	5.52	0.012	1.69	

^a Outliers were not considered for averages shown in Table 4 and Figures 4,6,7, and 8.

between the nakhlites and shergottites: Ce and V. Cerium shows a well-defined, expected increase in the nakhlites, but minimal variation in each shergottite (Fig. 3). When Ce is normalized to Y, as a proxy for the HREEs (Fig. 4), despite scatter, there does seem to be a decrease in the ratio between pyroxene cores and rims. A possible explanation for this is discussed below.

Vanadium also displays different behavior between the two lithologies, with a scattered, but definite, increase in the nakhlites and a decrease in the shergottites (Fig. 3). In this case, though, the nakhlite increase is unexpected. As reported by Rollinson (1993), V should behave as a compatible element in clinopyroxene (Table 1), which should produce a decreasing trend. Complicating the matter, however, the compatibility of V is susceptible to oxygen fugacity (Rollinson, 1993) and the crystallization of magnetite. The increase evident in the nakhlites, then, may reflect a difference in the oxidation state of the magma or in the timing of magnetite crystallization (i.e., much later crystallization of magnetite in the nakhlites), possibly making V less compatible than in the shergottites.

When the Li, Be, and B data are similarly plotted against TiO₂, again there are different behaviors between the nakhlites and shergottites (Fig. 5). Despite the scatter, it is apparent that

there is little variation, at scales comparable to the shergottites, in any of the three light lithophile elements in nakhlite pyroxenes. The shergottites, however, display both greater abundances and ranges in the light lithophile elements, with identifiable trends in the data: Be increases with TiO₂, whereas B and Li decrease.

4. INTERPRETATION OF LITHOPHILE ELEMENT ABUNDANCES

4.1. Data Quality

Because of the inherent difficulties of measuring and calibrating the light lithophile elements, we feel that a few checks on the quality of the data are warranted. For trace element data in the shergottites and the nakhlites, we can compare with data reported in Wadhwa et al. (1994) and Wadhwa and Crozaz (1995), respectively. The nakhlite data are all the same order of magnitude as those in Wadhwa and Crozaz (1995), with V, Zr, and Ce having identical or very similar values. Ti, and Y do display small offsets in values, with our concentrations being about twice that of Wadhwa and Crozaz (1995): e.g., Y = 4 to 8 ppm compared with 2 to 4 ppm. However, because the trends and spreads shown by these two elements are very similar, we believe the differences are due to interlaboratory variations and

Table 3. SIMS trace element data for pyroxenes (unless otherwise noted) in basaltic shergottites.

Specimen and site	TiO ₂ (wt%)	V (ppm)	Sr (ppm)	Y (ppm)	Zr (ppm)	Ce (ppm)	Li (ppm)	Be (ppm)	B (ppm)	Be (ppm) in plagioclase	
Shergotty											
px 1	Core (a) ^a	0.297	412	16.0	6.8	4.8	3.9	5.50	0.0013	3.64	0.062
	Midpoint (p) ^a	0.438	218	42.6	8.0	5.6	3.7	2.90	0.0031	2.80	0.063
	Rim (a)	0.774	54	50.7	8.5	34.2	3.6	1.89	0.0387	1.70	0.068
	Midpoint (a)	0.588	393	30.0	12.6	10.2	4.0	3.63	0.0032	2.65	0.062
	Rim (a)	0.798	75	49.4	8.6	24.0	3.6	2.45	0.0228	1.87	0.086
px 2	Core (p)	0.258	238	25.4	6.0	5.8	4.1	4.80	0.0058	7.24	0.055
	Rim (p)	0.671	164	51.4	8.7	21.7	3.7	2.64	0.0331	5.46	
px 3	Core (p)	0.436	236	32.8	8.3	7.2	3.9	5.19	0.0139	3.80	
	Rim (p)	0.628	61	51.3	8.0	17.9	3.5	1.98	0.0230	2.14	
px 4	Core (a)	0.304	425	17.3	7.0	4.6	4.0	8.15	0.0011	12.36	
	Rim (a) ^b	0.743	90	53.5	8.4	103.0	3.6	2.00	0.1623	3.36	
px 6	Core (a)	0.386	515	19.8	9.3	6.8	4.2	5.02	0.0026	9.75	
	Rim (p) ^b	0.599	41	61.8	6.2	31.8	3.5	1.68	0.1844	6.29	
	Rim (a)	0.675	67	49.1	7.8	15.5	3.6	1.78	0.0421	2.97	
Zagami											
px 1	Core (a)	0.390	529	22	9.0	8.1	5.6	7.87	0.017	3.23	0.117
	Rim (a) ^b	0.867	139	45	8.0	58.7	4.9	3.14	0.343	4.86	0.128
px 2	Core (a)	0.410	559	24	10.4	9.9	5.9	7.36	0.013	3.69	0.087
	Rim (a) ^b	0.641	333	41	9.8	35.3	5.3	6.21	0.199	4.72	0.095
px 3	Core (a)	0.422	505	29	10.4	10.1	5.5	7.16	0.019	3.68	0.075
	Rim (p) ^b	0.759	185	62	17.2	245.6	7.4	6.70	0.288	7.02	0.088
px 4	Core (a) ^{b,c}	0.815	208	46	13.5	95.7	6.3	4.09	0.111	4.64	
	Rim (p)	0.618	184	43	9.0	10.1	4.5	3.83	0.029	2.81	
px 8	Core (a)	0.362	417	28	8.4	9.4	5.4	6.92	0.019	5.90	
	Rim (p)	0.376	192	42	7.1	8.4	4.3	4.07	0.037	1.80	
px 10	Core (a)	0.379	506	21	8.9	7.3	5.0	6.99	0.013	3.13	
	Rim (a)	0.779	343	36	14.3	16.6	5.1	4.83	0.047	2.97	
px 13	Core (a)	0.328	432	33	7.5	11.4	6.2	8.00	0.012	8.81	
	Rim (a)	0.543	387	37	10.8	15.4	5.3	6.00	0.052	5.78	

^a a = augite, p = pigeonite, with an arbitrary boundary at Wo = 20 mol%.

^b Outliers were not considered for averages shown in Table 4 and Figures 4, 6, 7 and 8.

^c Plotted as open "rim" symbol in Figures 3 and 5 because compositionally they are more like rim material.

that the data are reliable for examining general element behavior. For the shergottite data, Wadhwa et al. (1994) present only graphical presentations of the Ti, Y, and Zr data and averages of their Ce data. Again, we find offsets in Ti, Y, and Zr but with similar trends and overlaps in values: e.g., Y = 5 to 15 ppm compared with 1 to 6 ppm (Wadhwa et al., 1994). Our Ce data show the most difference, with values an order of magnitude higher than the average in Wadhwa et al. (1994). Our measurements show that Zagami trace elements are roughly equivalent to those in Shergotty (same order of magnitude), as Wadhwa et al. (1994) also found.

The Li data seem reasonable when compared with the few bulk rock Li analyses in the literature (compiled by Meyer, 1998). We can generate a rough estimate for bulk Li by combining our average measurements with average modal abundances of pyroxene and plagioclase for Nakhla (Friedman Lentz et al., 1999), Shergotty (Hale et al., 1999), and Zagami (McCoy et al., 1992). We find that weighted sums of our Li analyses (4.5, 3.9, and 5.1 ppm, respectively) match well with previously reported bulk meteorite values (3.8, 3.3 to 5.6, and 3.8 ppm, respectively). There are no data in the literature with which to compare the B analyses, although we do find the same 10-fold difference between Shergotty pyroxene and maskelynite that Chaussidon and Robert (1999) reported. In addition, the lack of any serious spikes in B abundance, combined with our ion yield data, suggests that our anticontamination method

was successful and that those measured abundances, although slightly higher than expected, are reliable.

The other concern is Be, which has unexpectedly low abundances. The derived SIMS detection limit falls well below measured values, but to test the reliability of the data, we compared relative Be contents between plagioclase and pyroxene. If plagioclase and pyroxene had co-crystallized, their relative Be contents should reflect the Be distribution coefficients (Table 1): $D_{Be}(\text{plag/melt})/(\text{cpx/melt}) \sim 0.27/0.011 = 25$. It should be noted that there is a degree of imprecision in this ratio because distribution coefficients reported for Be are variable. For example, Brenan et al. (1998a) give a range of $D_{Be}(\text{cpx/melt})$ of 0.0025 to 0.021; we have chosen to use 0.011, which they report for a run involving Di composition.

In Shergotty and Zagami, the most similar conditions to equilibrium crystallization should have existed during the concurrent growth of pyroxene rims and interstitial plagioclase (Stolper and McSween, 1979). Shergotty and Zagami have similar average Be pl:px-rims ratios (2.1 and 2.4, respectively; see Table 4, Fig. 6), but these values are lower than the expected distribution coefficient ratio. Even the Be pl:px-cores (13 and 6, respectively; Table 4) are lower than the theoretical value, which is particularly unexpected. The core ratios should be higher than the theoretical value because the pyroxene cores grew well before plagioclase crystallization and would therefore have had less Be to incorporate than would have been

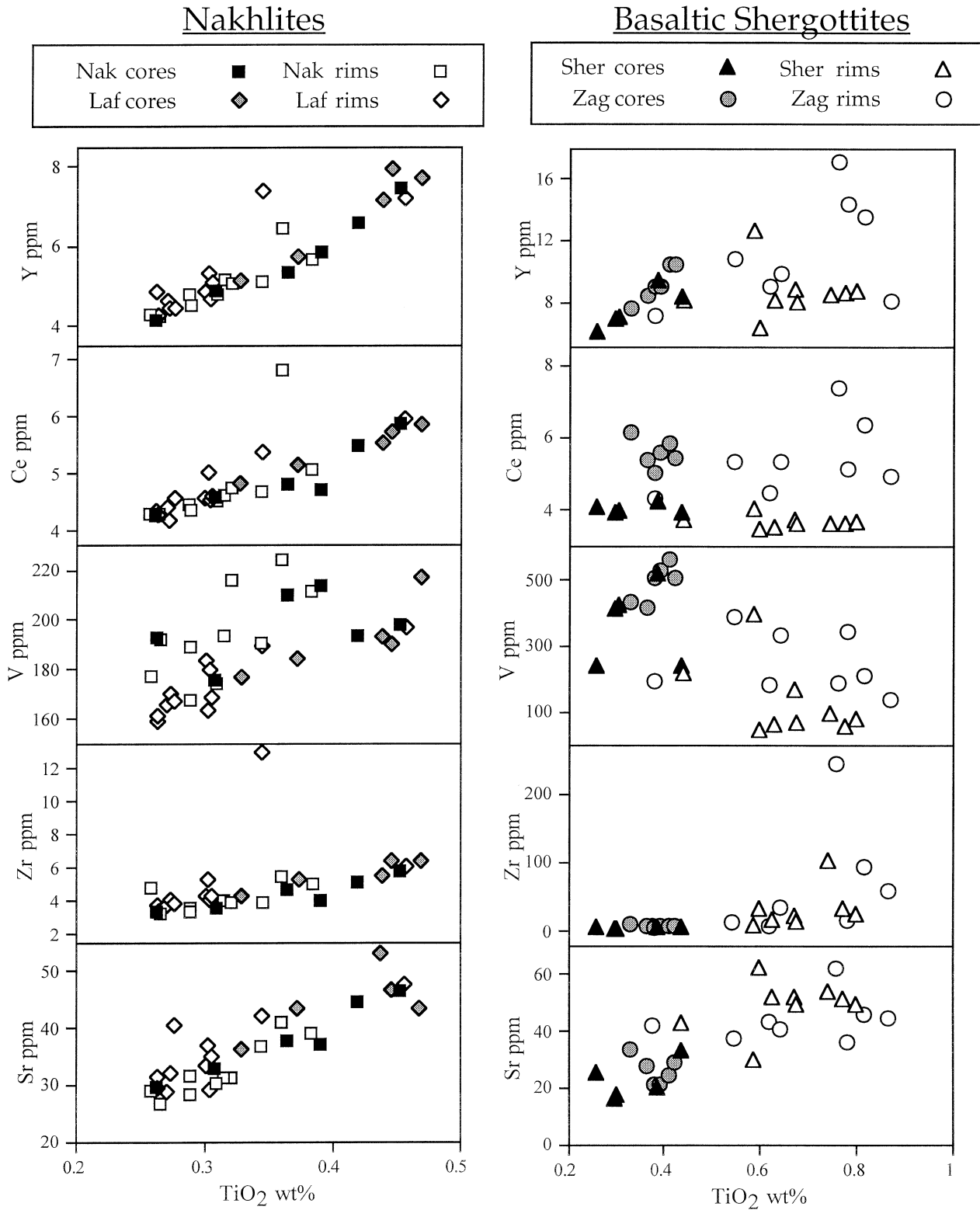


Fig. 3. Pyroxene trace element data (including outliers; see Table 3) for the nakhlites and basaltic shergottites. The expected incompatible and compatible trends are seen when plotted against TiO_2 , except for Ce in the shergottites and V in the nakhlites. See text for discussion.

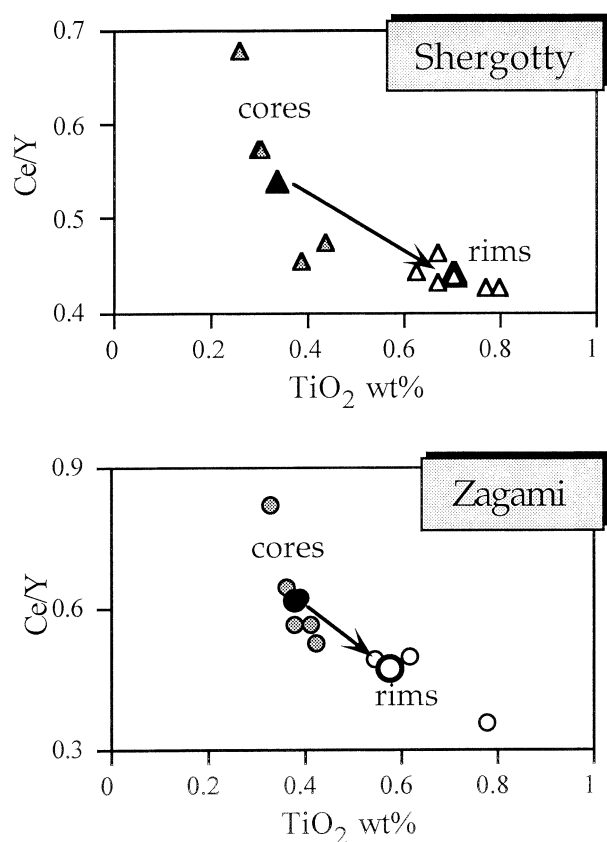


Fig. 4. Plots of Ce/Y vs. TiO₂ for shergottite pyroxenes (excluding outliers; see Table 3), with Y acting as a proxy for the HREEs, to illustrate an apparent Ce depletion from cores (gray filled symbols) to rims (open symbols). Larger symbols, connected by arrows, are averages for cores and rims.

available later. This expected late Be concentration is well displayed in the nakhlite data. In these meteorites, plagioclase grew very late with respect to pyroxene, within highly evolved melt pockets. Due to this magma evolution and incompatible element concentration, Be plagioclase to pyroxene ratios (both cores and rims) are quite high (Table 4, Fig. 6): ~ 100 to 400.

Although the nakhlite Be data fit our expectations, the shergottite data do not very well. One reason for this may be that we had to mix derived distribution coefficients from two sources: Brennan et al. (1998a) for pyroxene and Ryan (1989) for plagioclase. As such, there may be some discrepancies between the methods applied in the different studies, perhaps resulting in a higher D_{Be} (plag/melt) relative to D_{Be} (cpx/melt). Alternatively, the fact that the shergottite ratios are too low may be evidence of minor loss of Be during the shock-generated conversion of plagioclase to feldspathic glass. Despite the mixed results of this test, the Be data do show a distinct increase in abundance from pyroxene cores to rims to plagioclase, reflecting incompatible behavior. Because of this and the fact that the Be counts were well above the detection limit, we will proceed with the assumption that the data are sufficiently reliable for our examination of relative abundances of these light lithophile elements.

4.2. Elevated B Abundances and B/Be Ratios

A particularly interesting ratio to consider is that of B to Be. Because the ratio of distribution coefficients for B and Be in clinopyroxene is approximately equal to one ($D_B(\text{cpx/melt})/D_{Be}(\text{cpx/melt}) \sim 0.016/0.011 = 1.5$), the pyroxene core ratios, with only a minor adjustment, should approximate the starting ratios of those elements in the parent magmas. Our data (Table 4) show that the martian magmatic values are very high when compared with terrestrial basalt values (Fig. 7). For example, typical ocean island basalts (OIBs) have magmatic B/Be values of ~ 1 to 5 (Ryan et al., 1996), whereas nakhlite and Zagami core ratios average ~ 300 to 500. Shergotty has even higher pyroxene core B/Be ratios, averaging ~ 1500 (Table 4).

Elevated B/Be values in ocean island basalts have previously been attributed to low degrees of mantle melting that would enrich the B (Ryan et al., 1996). This mechanism seems unlikely here, though, as the very high martian values would require extremely low degrees of melting, given a starting composition similar to the terrestrial mantle. This would also run contrary to expected degrees of melting for shergottites and nakhlites on the basis of other trace elements (Wadhwa et al., 1994).

We suggest two other explanations, or possibly a combination of them. The B and Be contents of the martian mantle may simply be different from those of the Earth's mantle, with higher B relative to Be. Considering that B is much more volatile than Be, this would be consistent with the model of Dreibus and Wänke (1987), which suggests Mars was more volatile-rich after accretion.

Alternatively, contamination of magmas by surface materials could supply more B. The highest B/Be values (~ 200) found on Earth are in subduction zone arc lavas and have been attributed to addition of B from melting and dehydration of B-enriched ocean sediments on downgoing slabs. Because there is no evidence of such well-developed crustal recycling on Mars (Carr and Wänke, 1992), there would have to be some other mechanism than plate tectonics to mix crustal and mantle material. Two possibilities are crustal assimilation by the ascending magmas, or a well-developed groundwater system, to leach the crustal rocks and enrich the mantle magmas.

4.3. Boron and Lithium Depletions

Regardless of the source of the unexpectedly high B abundances, the relative differences that we see between pyroxene cores and rims in B and Li are of themselves intriguing (Fig. 8). In the nakhlites, Be, Li and B show minor increases (note scales), all behaving as incompatible elements would. This suggests that for most of the pyroxene crystallization, the three elements showed normal distribution behaviors.

The shergottite data are quite different. Be still increases from pyroxene cores to rims (Fig. 8), but both B and Li decrease from core to rim, on average. These decreases are more apparent in the Shergotty data, even considering 1σ errors, with the average values declining by more than 60%. The Zagami data are not as clear, especially the B, but there is a decided decrease, on average by $\sim 30\%$ (Fig. 8, Table 4). These trends suggest that between the time of pyroxene core and rim growth, B and Li were removed from the crystallizing

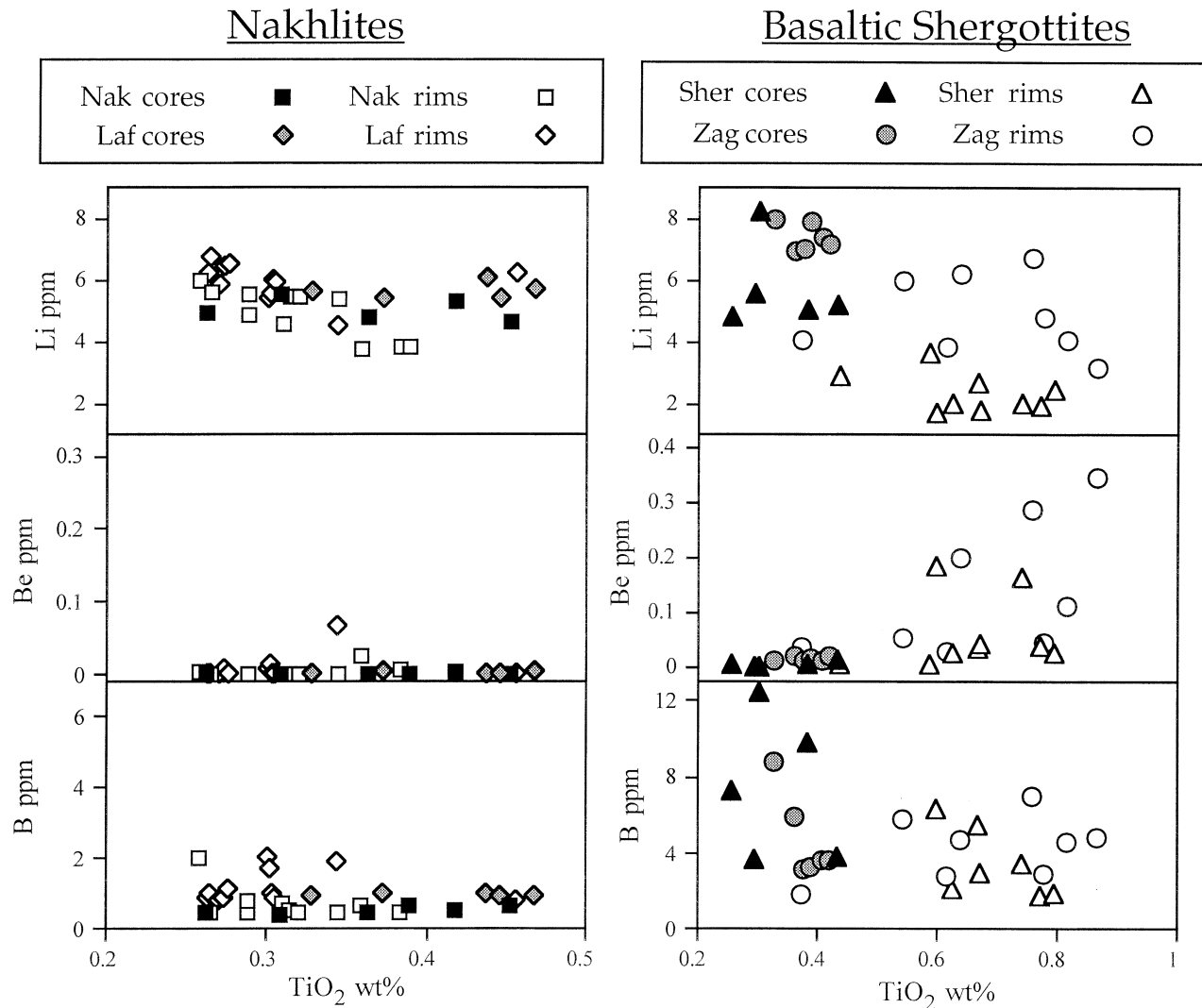


Fig. 5. Light lithophile element data (including outliers) for shergottite and nakhlite pyroxenes. Nakhlites show flat patterns (note scales for Be and B compared with those of the shergottites). Shergottites, despite scatter, show a general increase in Be, but decreases in Li and B, with increasing TiO₂.

magma. Because both B and Li are soluble in H₂O-rich hydrothermal fluids and Be is not, it seems reasonable to suggest that the loss of B and Li from the shergottite magmas occurred by a fluid-mediated process (i.e., exsolution and loss of a fluid from the melt during ascent).

Removal of Li and B in a fluid may be supported by a similar subtle decrease in Ce abundance, noted above (Fig. 4). Cerium is an unusual rare earth element (REE) in that it can exist in two oxidation states, Ce⁺³ and Ce⁺⁴. In a basaltic magma, Ce⁺³ should predominate because the presence of abundant Fe⁺² will reduce any Ce⁺⁴ (Neal and Taylor, 1989). Trivalent Ce has been suggested to be more soluble than other trivalent REEs in hydrothermal fluids, and much more so than Ce⁺⁴. This leads to negative Ce anomalies in hydrothermally altered subduction zone lavas (e.g., Ludden and Thompson, 1979) and positive Ce anomalies in nodules precipitated from oxidized fluids (e.g., Elderfield et al., 1981). The depletion seen in Ce, then, when

compared with Y (as a heavy REE proxy), may be consistent with the scenario of an exsolving hot fluid removing particularly soluble species from the magma and being lost, between the times of pyroxene core and rim growth. However, it should be noted that Ce data for Shergotty and Zagami presented by Wadhwa et al. (1994) contradict this finding, showing an increase from pyroxene cores to rims.

5. DISCUSSION

5.1. Eruption Scenario

Previous studies of shergottite pyroxene compositions and crystal size distributions (e.g., Stolper and McSween, 1979; McCoy et al., 1992; Lentz and McSween, 2000) have concluded that Shergotty and Zagami had multistage crystallization histories. Most likely, Mg-rich pyroxene cores formed at depth, and the compositional shift to Fe-rich rims occurred

Table 4. Pyroxene and plagioclase averages and ratios.

Sample	TiO ₂ (wt%)	Ce (ppm)	Li (ppm)	Be (ppm)	B (ppm)	Plagioclase Be/px Be	Average B/Average Be ^a
Nakhla							
px Cores	0.37	5.0	4.8	0.001	0.55	392	472
px Rims ^b	0.31	4.6	5.1	0.002	0.79	234	
Plagioclase	0.13	7.8	1.1	0.45	5.1		
Lafayette							
px Cores	0.41	5.4	5.6	0.002	0.95	301	527
px Rims ^b	0.29	4.5	6.1	0.005	1.29	106	
Plagioclase	0.17	25	0.6	0.54	6.4		
Shergotty							
px Cores	0.34	4.0	5.7	0.005	7.4	13.4	1495
px Rims ^b	0.71	3.6	2.1	0.032	2.8	2.1	
Plagioclase	0.134	4.16	6.0	0.07	0.50		
Zagami							
px Cores ^b	0.38	5.6	7.4	0.016	4.7	6.3	303
px Rims ^b	0.58	4.8	4.7	0.041	3.3	2.4	
Plagioclase	0.134	4.51	4.7	0.10	0.59		

^a These values were divided by 1.5 in Figure 7 to better approximate magmatic values.

^b Selected averages not including outliers identified in Tables 2 and 3.

upon eruption of the magma or its injection as a shallow sill. Our interpretation of water loss between these two growth periods seems to fit well with this hypothesis. However, for this water loss to be a valid explanation of the Li and B decreases, we must explore the likelihood of such a scenario.

We envision the following eruption scenario for the case of a wet parent magma. At depth, the water component would remain in solution in the magma due to the confining pressure. The Mg-rich cores growing at depth would thus reflect the starting B and Li abundances of the magma (Fig. 9a). During magma ascent, material with the Mg-rich composition could

continue to crystallize (Lentz and McSween, 2000), but at some critical depth, with a drop in confining pressure, the volatile component would begin to exsolve from the magma. A gradual exsolution of the volatile phase during ascent would progressively dissolve the soluble species from the magma, leaving less B and Li for incorporation into crystallizing pyroxene (Fig. 9b). This would explain the incremental depletion we see in a traverse of a Shergotty pyroxene grain (Fig. 10).

Where would the volatile component go? With exsolution of a significant volume of volatiles and continued magma ascent, a magma will often reach the point where the confining pressure is no longer sufficient to contain the volatile bubbles, and disruption of the magma will occur (e.g., Wilson and Head, 1981). Depending on the volatile contents and the magma ascension rate, this may occur at the surface or at some shallow depth, in which case overlying country rock may also be

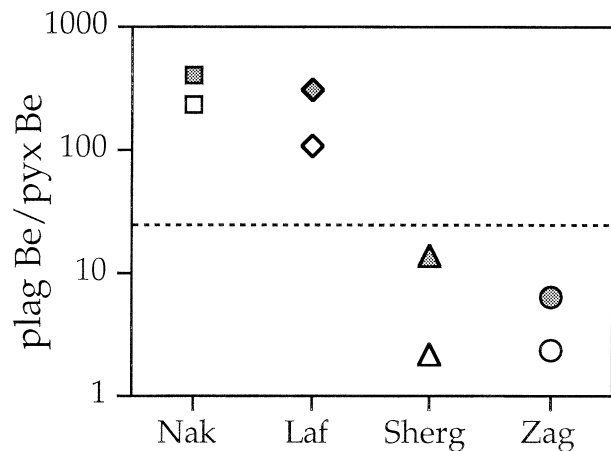


Fig. 6. Ratios of Be abundances in plagioclase (or plagioclase glass) and pyroxene (note log scale) for the martian meteorites analyzed. Dashed line represents the ratio expected, from relative distribution coefficients, if plagioclase and pyroxene grew in equilibrium. Solid symbols show average ratio with pyroxene core values; open symbols show average rim data. Shergottite ratios fall below expected ratio, despite nearly concurrent growth of plagioclase and pyroxene rims, perhaps indicating minor losses of Be during shock-generated conversion of plagioclase to feldspathic glass. Nakhilites, with late stage plagioclase growth, show very high ratios due to concentration of Be in the evolved melt pockets. Errors are smaller than symbols.

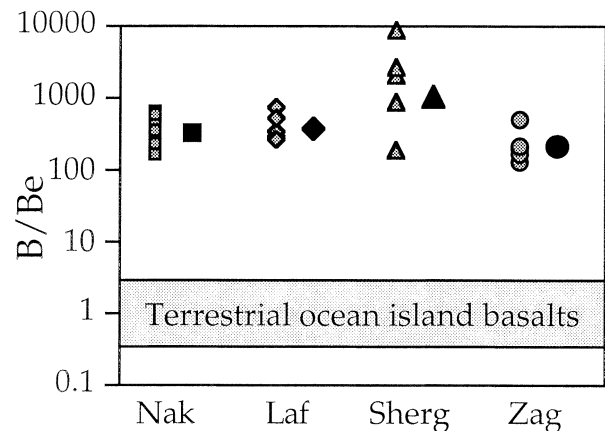


Fig. 7. Boron to Be ratios for pyroxene cores in martian meteorites, with averages (larger symbols). Because clinopyroxene B and Be distribution coefficients are nearly equal ($D_B/D_{Be} = 1.5$), slightly adjusted core ratios approximate magmatic ratios. Note the high martian ratios compared with typical terrestrial ocean island basalt values (Ryan et al., 1996).

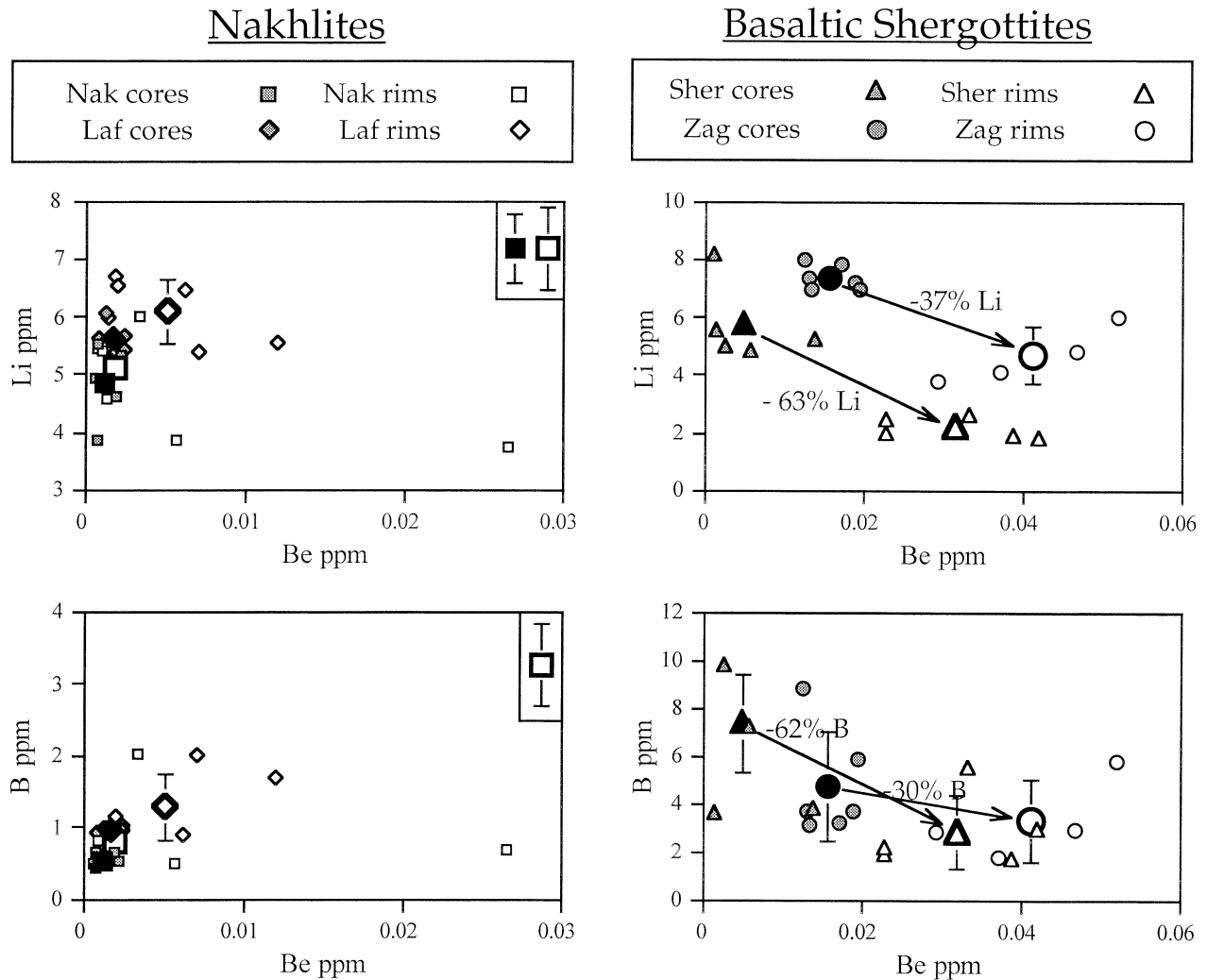


Fig. 8. Li and B pyroxene data plotted vs. Be (excluding outliers), to emphasize the differences between the nakhlites and shergottites. Note that the scale on B nakhlite graphs is half that of the shergottite graph. Large symbols are average values. Be increases in all cases from cores to rims. In the nakhlites, Li and B increase marginally, but in the shergottites, they decrease substantially, and consistently, within each meteorite, as noted by percent decreases. 1σ error bars are included for average values. Where not visible, error is smaller than symbol.

disrupted. Devolatilization would be accentuated on Mars, relative to Earth, due to the planet's lower gravity and thus lower confining pressure (Mouginis-Mark et al., 1991). However, there is no petrographic evidence, such as incorporated quenched fragments, that the Shergotty or Zagami magmas underwent a disruptive phase (e.g., fire fountaining). We can speculate, though, that the accumulated volatile contents could have risen more quickly through the low-viscosity magma column and ultimately disrupted only the uppermost levels of the magma body (Fig. 9c). If such were the case, then the rocks we now examine, with the telltale B and Li depletions, could have crystallized from magma originating deeper within the column. This remaining volatile-depleted magma would have continued to rise and eventually erupted less violently onto the surface (Fig. 9d). Plagioclase and Fe-rich pyroxene rims thought to have grown postemplacement would then display depletions in the soluble species (Table 4).

5.2. Solubility Issues

The likelihood of this suggested sequence of events is dependent on the dissolution of the soluble elements in an aqueous fluid. In calling upon this mechanism, we must consider a couple of factors. First, we must assume that the conditions during exsolution of the volatile phase were appropriate for the aqueous component to exsolve as a fluid, rather than a vapor. If water were the only component, this would be a reasonable assumption. The likely pressure and temperature conditions at the time of volatile exsolution would have been well above the critical point for H_2O , suggesting an aqueous component would exsolve for a considerable period as a supercritical fluid. Only late in the ascent process would the confining pressure drop to the point of causing the supercritical fluid to become a true vapor. An observation that may support this idea is the fact that late-stage pyroxene rims and plagioclase, both thought to have

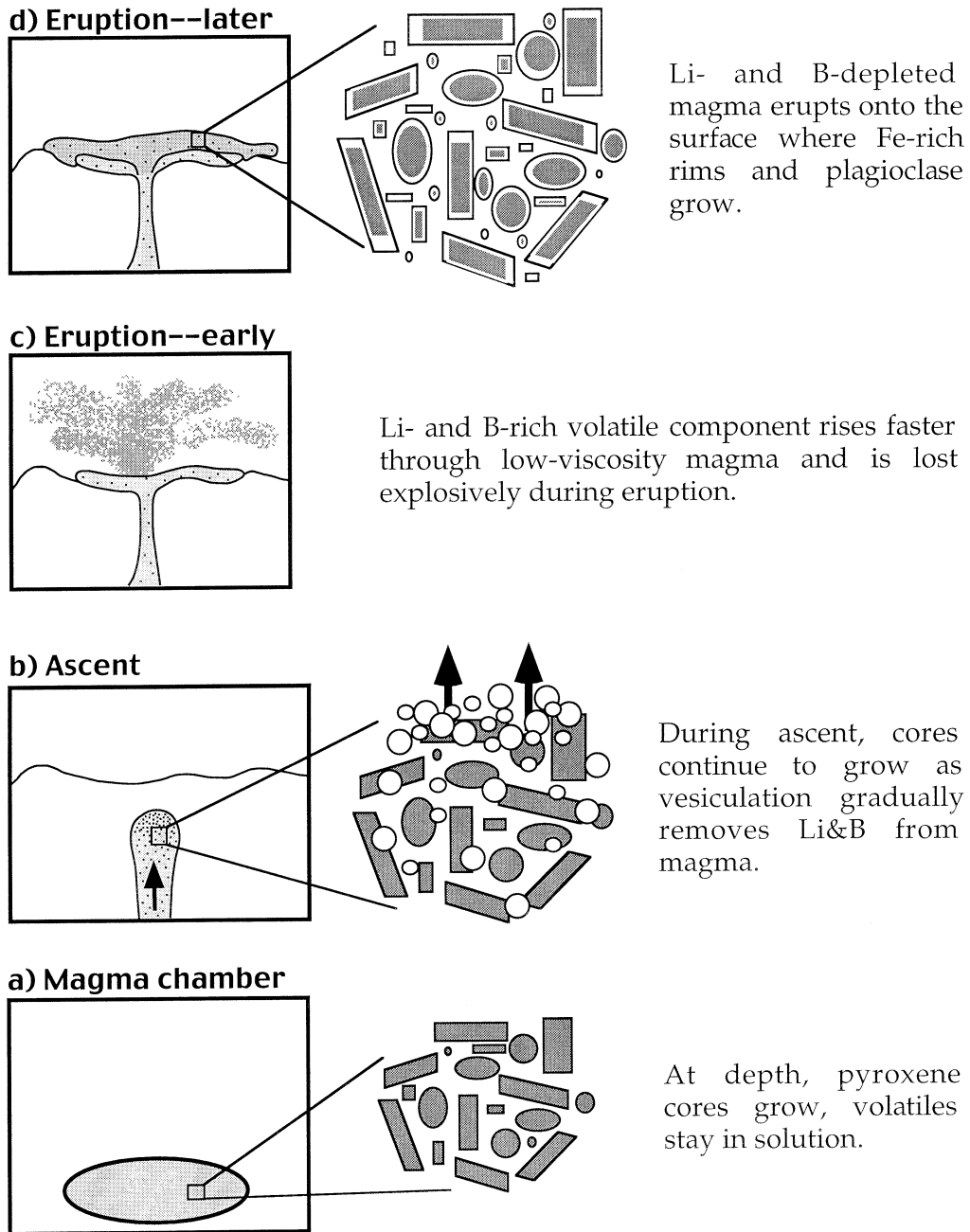


Fig. 9. Schematic depicting a scenario of volatile exsolution during ascent and degassing at the surface to explain the loss of soluble elements in the shergottites between pyroxene core crystallization at depth and rim growth near or on the surface.

grown postemplacement, do still contain some amounts of the soluble species: at shallow depths, the remaining volatile component might have exsolved in the vapor state, hampering dissolution of the remaining B and Li in the magma. However, it should be noted that there may well have been other volatile species involved, such as CO_2 or SO_2 , that could have had an affect on the phase state of the aqueous component and on its solubility in the magma. Because we do not know how much of which other volatile species were present, we can not know for certain whether most of the water exsolved as a fluid phase.

Another aspect relevant to the solubility issue is the coordination state of the boron. All B bound in silicate materials is tetrahedrally coordinated, serving as a poor substitute for Si. In hydrous fluids, B speciation is a function of pH (Kakihana et al., 1977), with trigonal coordinated B favored as pH declines. In the case of the shergottites, the magmas were probably quite acidic, and any exsolved fluid would likely have been acidic as well. Therefore, the removal of B from the acidic melt to the acidic volatile component need not have involved any change of coordination state, so probably did not affect B solubility. On the other hand, leaching of B from already crystallized

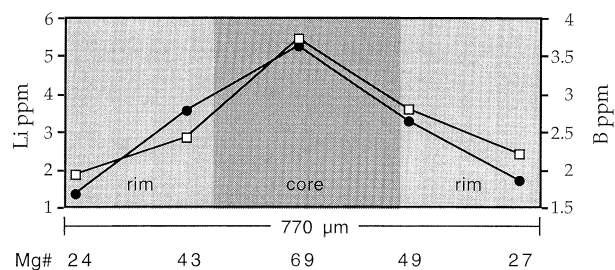


Fig. 10. Shergotty pyroxene traverse of Li (open squares) and B (filled circles) abundances illustrating gradual depletion of these soluble elements from core to rim. Mg#s for analyzed spots are shown below the graph.

pyroxene would probably have been hampered by the necessary coordination state change and thus be less likely to occur.

In evaluating the likelihood of our dissolution scenario, we must also consider the fact that the depletions of Li and B are in about the same proportion (~60% in Shergotty, ~30% in Zagami). This is unexpected when their solubilities are examined (Table 1). On the basis of the distribution coefficients of the elements between a melt and fluid, one would expect much greater concentrations of Li to have been removed, compared with B. A possible explanation for this lies in the fact that diffusion rates of Li in alkali feldspars are quite high (Giletti and Shanahan, 1997). Although pyroxene has a different crystal structure than feldspars, Li may still have the tendency to diffuse readily in other silicates, like pyroxene. In such a case, more Li may actually have been removed from the melt, generating a steeper profile across pyroxene grains. During postemplacement cooling, however, a degree of diffusive equilibration could have smoothed out the core-rim discrepancy in Li to a level similar to that of B.

5.3. Depth Calculations

If dissolution and removal by water is the source of the B and Li depletions, the relative decrease of each element suggests a significant amount of water was lost, although quantifying this amount with our data alone is not possible. However, recent experimental work (Dann et al., 2001), supports our hypothesis of a wet parent magma for Shergotty, suggesting that there may have been ~1.8 wt% dissolved water at depth. Dann et al. (2001) focused on experimentally reproducing Shergotty pyroxene compositions and found that the conditions that yielded the best match for co-crystallizing pigeonite and augite core compositions were at water pressures of 40 to 50 MPa. With this information and the two-stage growth models, we can use water solubility information to constrain rough estimates of the depths of crystallization for pyroxene cores and rims.

In calculating the depth of H₂O exsolution, we employed two different water solubility estimates, both assuming that water is the only volatile in question. (If other volatile species were present this would, of course, affect the solubility curves, but with no constraints on these other species we present this as a first-order estimate.) The first uses an empirical equation presented by Wilson and Head (1981) for water solubility in basalt, which is based on experimental data of Mysen (1977). The second is a more recent, and complex, relationship derived

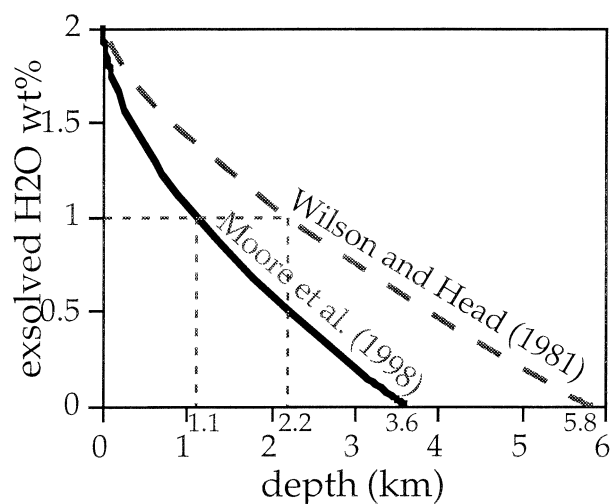


Fig. 11. Calculated water exsolution profiles for 2 wt% water in a basaltic magma on Mars. The two governing equations for water solubility (Wilson and Head, 1981; Moore et al., 1998) are based on different experimental data sets, but show the same gradual exsolution of water with decreasing depth. Shergotty cores would have formed below the depth where water began to exsolve, whereas the rims probably formed at some depth shallower than ~0.5 km, if not on the surface.

by Moore et al. (1998), based on their own experimental results and depending on the specific melt composition as well as pressure, temperature, and water fugacity. Both methods give a solubility reflecting pressure (in bars), which we convert into depth by using the relationship

$$\text{Pressure} = \rho_{\text{crust}} \times g \times h$$

where we use appropriate values for Mars ($\rho_{\text{crust}} = 3000 \text{ kg/m}^3$, $g_{\text{Mars}} = 3.728 \text{ m/s}^2$).

Both solubility calculations show that there is a progressive decrease in dissolved water over a depth interval of several kilometers (Fig. 11). This seems consistent with our findings of a gradual depletion of Li and B in measured profiles (Fig. 10). Because neither Shergotty nor Zagami contain vesicles, and both meteorites are quite dry now, for the purposes of this calculation, we will assume that virtually all the water exsolved by the time of eruption. This would imply that the water began to exsolve at ~4 to 6 km, which would define minimum depths for the crystallization of the pyroxene cores. Furthermore, if we equate the relative amounts of element lost to water lost, the solubility curves suggest that the Shergotty rim compositions, with losses of well over half the B and Li, crystallized at depths of <0.5 km. This would be consistent with previous interpretations of shallow or surface growth of pyroxene rims (e.g., McCoy et al., 1992; Lentz and McSween, 2000).

5.4. Source of Magmatic Water

If these magmas did contain, and then lose, substantial amounts of water, the source of that water is important. Would its presence imply a mantle source region containing significant quantities of water? The conventional view of a volatile-rich but dry martian mantle was developed by Dreibus and Wänke

(1987). In their model, a mantle water content of 36 ppm was determined from the abundances and relative solubilities of H₂O and Cl in basaltic magma. However, Lodders and Fegley (1997) argued that this method does not hold for the terrestrial mantle, underestimating water abundances in the mantle because of the concentration of Cl in the Earth's crust. They suggested that Cl may likewise have been sequestered in the martian crust, an idea bolstered by the high measured concentrations of Cl in martian soils (Rieder et al., 1997). In fact, Lodders and Fegley (1997) derived a bulk Mars Cl abundance eight times higher than that of Dreibus and Wänke (1987), with a correspondingly higher mantle water content.

However, it seems more likely that any water in the Shergotty and Zagami magmas would have derived from the crust. Leshin (2000) recently determined that D/H values measured in an apatite grain of QUE 94201 suggest a martian crust two to three times wetter than previously thought, providing a good source for the water. Different degrees of crustal contamination in the martian meteorites have been suggested on the basis of a trend of trace element and radiogenic isotope values, with Shergotty and Zagami falling at one end. The measured LREE enrichment, high initial ⁸⁷Sr/⁸⁶Sr and low initial ¹⁴³Nd/¹⁴⁴Nd isotopic compositions (Jones, 1989; Longhi, 1991), and relatively high oxidation states (Herd and Papike, 2000) of these meteorites suggest modification from mantle values, as typified by the QUE 94201 shergottite (Borg et al., 1997). Whether this crustal contaminant was a fluid or a hydrated rock is unknown, but either would tie in well with our speculations on the high B values discussed above. In addition, if our calculated depths of >4 km for pyroxene core growth are correct, this may imply deep circulation of groundwater to hydrate the crust to such depths.

5.5. Shergotty vs. Zagami

The overall scenario we propose for Shergotty is likely similar for Zagami, as it shows the same depletions in soluble elements as Shergotty. However, where Shergotty has lost ~60% of B and Li between growth of pyroxene cores and rims, Zagami has lost only ~30%. To what is this difference attributable?

The simplest explanation may be that the cores we analyzed in Zagami were not the innermost core material. It is unlikely that cuts directly through pyroxene cores were made, especially with the smaller pyroxene grains in Zagami. The Zagami pyroxene cores analyzed in this study had Mg#s ranging from 42 to 52, whereas those analyzed by McCoy et al. (1999) and Stolper and McSween (1979) ranged from 66 to 71. This would imply that the most primitive core compositions were not measured, resulting in an apparently smaller decrease in light lithophile elements between pyroxene cores and rims.

However, the finer grain size of Zagami suggests that there must have been some difference in the crystallization histories between the two shergottites, and this may also have influenced the loss of soluble elements. Grain size data (Lentz and McSween, 2000) show that the average size of Zagami pyroxene grains, cores plus rims, is nearly identical to the average size of Shergotty pyroxene cores. Those authors speculated that the Mg-rich cores in Shergotty actually represent two phases of growth: one at depth in a magma chamber, and the other as the

magma ascended. To generate the smaller Mg-rich cores in Zagami, then, perhaps only one of these growth phases occurred: either crystallization at depth with no further core growth during a faster ascent than Shergotty, or no crystallization at depth but nucleation and growth of the cores during ascent. In either case, Mg-rich cores of similar composition to those in Shergotty were still produced but did not grow as large before conditions changed to crystallization of Fe-rich rims. Faster cooling at (or near) the surface may also have been a factor in producing thinner rims and smaller overall grain sizes. As regards the light lithophile elements, in either scenario (core growth at depth with a rapid ascent or core growth en route), Zagami would have experienced a shorter period of exsolution and thereby less removal of B and Li.

6. CONCLUSIONS

We have examined the relative abundances of the light lithophile elements Li, Be and B in minerals of martian meteorites, which until now have been virtually unstudied. In Nakhla and Lafayette, the elements show increases, even if minimal, as we would expect for incompatible elements, suggesting little, if any, magmatic water interaction. Shergotty and Zagami, on the other hand, display a loss of soluble Li and B between growth of pyroxene cores and rims, where other incompatible elements like Be, Y, Zr, Sr, and Ti show the expected increases with fractional crystallization. In conjunction with new experimental petrology results (Dann et al. 2001), this leads us to suggest that the parent magmas for Shergotty and Zagami may have had significant water contents that were lost by exsolution during ascent and degassing upon extrusion.

Magmatic B/Be ratios in these four martian meteorites are uniformly higher than any terrestrial basaltic values, consistent with a volatile-rich martian mantle. However, whether this indicates a wet mantle is still unclear. Although the source of any water for the shergottite parent magmas could be the mantle, trace element and isotopic evidence suggests Shergotty and Zagami contain a significant component of crustal contamination, implying that magmatic water could also have been derived by assimilation of crustal materials. Such contamination could also explain the elevated B values we measured.

Regardless of the ultimate water source, solubility calculations suggest that if the shergottite magma was wet, the pyroxene cores may have crystallized at depths of >4 km where water would have been dissolved in the magma. During ascent of the magma, water could gradually exsolve, removing soluble elements from the melt. Upon eruption, this H₂O-rich volatile component could have degassed, leaving the B- and Li-depleted magma to crystallize pyroxene rims and plagioclase. Zagami shows similar compositional trends to Shergotty, with depletions of the soluble elements in pyroxene rims and plagioclase, but only by half as much. This lesser depletion, combined with smaller pyroxene core and overall grain sizes, suggests the Zagami magma either ascended more rapidly, or core growth actually began at shallower depths once the magma was ascending. In either case, the Zagami magma would have undergone less volatile exsolution and loss of soluble elements.

This work presents a possibility for reconciling geochemical

evidence for magmatic water in martian volcanic rocks with geologic evidence for surface water in middle and late martian time. Extrapolation of the Shergotty and Zagami results to global martian volcanism is debatable, although visible/near-infrared spectra suggest that shergottite-like basalts may be common on the planet's surface (Mustard et al., 1997). Certainly, the possibility of significant magmatic water, combined with the young (~175 Ma) crystallization ages (Jones, 1986) of these meteorites, raises a compelling mechanism for delivering water to the martian surface during recent volcanism.

Acknowledgments—We thank Tim McCoy (Smithsonian) and Rhian Jones (University of New Mexico) for the generous loan of samples for this study. Lionel Wilson and Gordon Moore provided input on water solubility in basalts, and Ed Stolper offered thought-provoking comments on B solubility issues. The manuscript was improved by thoughtful reviews from Jim Webster, Gerlind Dreibus, and an anonymous reviewer. This work was supported by NASA grant NAG 54541 to H.Y.M. and by the Office of Basic Energy Science, U.S. Department of Energy under contract DE-AC05-00OR22725 with Oak Ridge National Laboratory, managed by UT-Battell, LLC, to L.R.R.

Associate editor: H. Palme

REFERENCES

- Borg L. E., Nyquist L. E., Taylor L. A., Wiesmann H., and Shih C.-Y. (1997) Constraints on martian differentiation processes from Rb-Sr and Sm-Nd isotopic analyses of the basaltic shergottite QUE94201. *Geochim. Cosmochim. Acta* **61**, 4915–4931.
- Brenan J. M., Neroda E., Lundstrom C. C., Shaw H. F., Ryerson F. J., and Phinney D. L. (1998a) Behaviour of boron, beryllium, and lithium during melting and crystallization: Constraints from mineral-melt partitioning experiments. *Geochim. Cosmochim. Acta* **62**, 2129–2141.
- Brenan J. M., Ryerson F. J., and Shaw H. F. (1998b) The role of aqueous fluids in the slab-to-mantle transfer of boron, beryllium, and lithium during subduction: Experiments and models. *Geochim. Cosmochim. Acta* **62**, 3337–3347.
- Carr M. H. and Wänke H. (1992) Earth and Mars: Water inventories as clues to accretional histories. *Icarus* **98**, 61–71.
- Chaussidon M. and Robert F. (1999) $^7\text{Li}/^6\text{Li}$ and $^{11}\text{B}/^{10}\text{B}$ ratios of SNC meteorites Chaussidon M. and Robert F. (1999) $\text{Fli}/6\text{Li}$ and $^{11}\text{B}/^{10}\text{B}$ ratios of SNC meteorites. In Lunar and Planetary Science XXX, Abstract #1592, Lunar and Planetary Institute, Houston (CD-ROM).
- Dann J. C., Holzheid A. H., Grove T. L., and McSween H. Y. Jr. (2001) Phase equilibria of the Shergotty meteorite: Constraints on pre-eruptive H_2O contents of martian magmas and fractional crystallization under hydrous conditions. *Meteorit. Planet. Sci.* **36**, 793–806.
- Dreibus G. and Wänke H. (1987) Volatiles on Earth and Mars: A comparison. *Icarus* **71**, 225–240.
- Elderfield H., Hawkesworth C. J., Greaves M. J., and Calvert S. E. (1981) Rare earth element geochemistry of oceanic ferromanganese nodules and associated sediments. *Geochim. Cosmochim. Acta* **45**, 513–528.
- Floran R. J., Printz M., Hlava P. F., Keil K., Nehru C. E., and Hinthorne J. R. (1978) The Chassigny meteorite: A cumulate dunite with hydrous amphibole-bearing melt inclusions. *Geochim. Cosmochim. Acta* **42**, 1213–1229.
- Friedman Lentz R. C., Taylor G. J., and Treiman A. H. (1999) Formation of a martian pyroxenite: A comparative study of the nakhlite meteorites and Theo's Flow. *Meteorit. Planet. Sci.* **34**, 919–932.
- Giletti B. J. and Shanahan T. M. (1997) Alkali diffusion in plagioclase feldspar. *Chem. Geol.* **139**, 3–20.
- Hale V. P. S., McSween H. Y. Jr., and McKay G. A. (1999) Re-evaluation of intercumulus liquid composition and oxidation state for the Shergotty meteorite. *Geochim. Cosmochim. Acta* **63**, 1459–1470.
- Harvey R. P. and McSween H. Y. Jr. (1992) Petrogenesis of the nakhlite meteorites: Evidence from cumulate mineral zoning. *Geochim. Cosmochim. Acta* **56**, 1655–1663.
- Head J. W. III, Hiesinger H., Ivonov M. A., Kreslavsky M. A., Pratt S., and Thomson B. J. (1999) Possible ancient oceans on Mars: Evidence from Mars Orbiter laser altimeter data. *Science* **286**, 2134–2137.
- Herd C. D. K. and Papike J. J. (2000) Oxygen fugacity of the martian basalts from analysis of iron–titanium oxides: Implications for mantle–crust interaction on Mars (abstract). *Meteor. Planet. Sci.* **35**, A70.
- Johnson M. C., Rutherford M. J., and Hess P. C. (1991) Chassigny petrogenesis: Melt compositions, intensive parameters, and water contents of martian (?) magmas. *Geochim. Cosmochim. Acta* **55**, 349–366.
- Jones J. H. (1986) A discussion of isotopic systematics and mineral zoning in the shergottites: Evidence for a 180 my igneous crystallization age. *Geochim. Cosmochim. Acta* **50**, 969–977.
- Jones J. H. (1989) Isotopic relationships among the shergottites, the nakhlites and Chassigny. *Proc. Lunar Planet. Sci. Conf.* **19**, 465–474.
- Kakihana H., Kotaka M., Satoh S., Nomura M., and Okamoto M. (1977) Fundamental studies of the ion exchange separation of boron isotopes. *Bull. Chem. Soc. Jpn.* **50**, 158–163.
- Karllson H. R., Clayton R. N., Gibson E. K. Jr., and Mayeda T. K. (1992) Water in SNC meteorites: Evidence for a martian hydrosphere. *Science* **255**, 1409–1411.
- King P. L., Hervig R. L., Holloway J. R., Vennemann T. W., and Righter K. (1999) Oxy substitution and dehydrogenation in mantle-derived amphibole megacrysts. *Geochim. Cosmochim. Acta* **63**, 3635–3651.
- Lentz R. C. F. and McSween H. Y. Jr. (2000) Crystallization of the basaltic shergottites: Insights from crystal size distribution (CSD) analysis of pyroxenes. *Meteorit. Planet. Sci.* **35**, 919–927.
- Leshin L. A. (2000) Insights into martian water reservoirs from analyses of martian meteorite QUE 94201. *Geophys. Res. Lett.* **27**, 2017–2020.
- Lodders K. and Fegley B. Jr. (1997) An oxygen isotope model for the composition of Mars. *Icarus* **126**, 373–394.
- Longhi J. (1991) Complex magmatic processes on Mars: Inferences from the SNC meteorites. *Proc. Lunar Planet. Sci. Conf.* **21**, 695–709.
- Ludden J. N. and Thompson G. (1979) An evaluation of the behaviours of the rare earth elements during the weathering of sea-floor basalt. *Earth Planet. Sci. Lett.* **43**, 85–92.
- Malin M. C. and Edgett K. S. (2000) Evidence for recent groundwater seepage and surface runoff on Mars. *Science* **288**, 2330–2335.
- McCoy T. J., Taylor G. J., Keil K. (1992) Zagami: Product of a two-stage magmatic history. *Geochim. Cosmochim. Acta* **56**, 3571–3582.
- McCoy T. J., Wadhwa M., Keil K. (1999) New lithologies in the Zagami meteorite: Evidence for fractional crystallization of a single magmatic unit on Mars. *Geochim. Cosmochim. Acta* **63**, 1249–1262.
- McKay D. S., Gibson E. K. Jr., Thomas-Keprta K. L., Vali H., Romanek C. S., Clemett S. J., Chillier X. D. F., Maechling C. R., and Zare R. N. (1996) Search for past life on Mars: Possible relic biogenic activity in martian meteorite ALH84001. *Science* **273**, 924–930.
- McSween H. Y. Jr. and Harvey R. P. (1993) Outgassed water on Mars: Constraints from melt inclusions in SNC meteorites. *Science* **259**, 1890–1892.
- Measures C. I. and Edmond J. M. (1983) The geochemical cycle of ^9Be : A reconnaissance. *Earth Planet. Sci. Lett.* **66**, 101–110.
- Meyer C. (1998) Mars meteorite compendium—1998. Updated August 6, 1998. Available at: <http://www-curator.jsc.nasa.gov/curator/antmet/mmc/mmc.htm>. Accessed September 14, 2001.
- Moore G., Vennemann T., and Carmichael I. S. E. (1998) An empirical model for the solubility of H_2O in magmas to 3 kilobars. *Am. Mineral.* **83**, 36–42.
- Mouginis-Mark P. J., Wilson L., and Zuber M. T. (1991) The physical volcanology of Mars. In *Mars* (eds. H. H. Kieffer et al.), pp. 424–452. University of Arizona Press.
- Mustard J. F., Murchie S., Erard S., and Sunshine J. M. (1997) In situ compositions of martian volcanics: Implications for the mantle. *J. Geophys. Res.* **102**, 25605–25615.
- Mysen B. O. (1977) The solubility of H_2O and CO_2 under predicted

- magma genesis conditions and some petrological and geophysical implications. *Rev. Geophys. Space Phys.* **15**, 351–361.
- Neal C. R. and Taylor L. A. (1989) A negative Ce anomaly in a peridotite xenolith: Evidence for crustal recycling into the mantle or mantle metasomatism? *Geochim. Cosmochim. Acta* **53**, 1035–1040.
- Noll P. D. Jr., Newsom H. E., Leeman W. P., and Ryan J. G. (1996) The role of hydrothermal fluids in the production of subduction zone magmas: Evidence from siderophile and chalcophile trace elements and boron. *Geochim. Cosmochim. Acta* **60**, 587–611.
- Popp R. K., Virgo D., Yoder H. S. Jr., Hoering T. C., and Phillips M. W. (1995) An experimental study of phase equilibria and Fe oxy-component in kaersutitic amphibole: Implications for the f_{H_2} and $a_{\text{H}_2\text{O}}$ in the upper mantle. *Am. Mineral.* **80**, 534–548.
- Rieder R., Economou T., Wanke H., Turkevich A., Crisp J., Bruckner J., Dreibus G., and McSween H. Y. Jr. (1997) The chemical composition of martian soil and rocks returned by the mobile alpha proton x-ray spectrometer: Preliminary results from the x-ray mode. *Science* **278**, 1771–1774.
- Rollinson H. (1993) *Using Geochemical Data: Evaluation, Presentation, Interpretation*. Longman Geochemistry Series. Longman Group.
- Ryan J. G. (1989) The systematics of lithium, beryllium, and boron in young volcanic rocks. Ph.D. Dissertation, Columbia University.
- Ryan J. G. (2002) The trace-element systematics of beryllium in geologic systems. *Rev. Mineral.*, in press.
- Ryan J. G. and Langmuir C. H. (1987) The systematics of lithium abundances in young volcanic rocks. *Geochim. Cosmochim. Acta* **51**, 1727–1741.
- Ryan J. G. and Langmuir C. H. (1988) Beryllium systematics in young volcanic rocks: Implications for ^{10}Be . *Geochim. Cosmochim. Acta* **52**, 237–244.
- Ryan J. G. and Langmuir C. H. (1993) The systematics of boron abundances in young volcanic rocks. *Geochim. Cosmochim. Acta* **57**, 1489–1498.
- Ryan J. G., Leeman W. P., Morris J. D., and Langmuir C. H. (1996) The boron systematics of intraplate lavas: Implications for crust and mantle evolution. *Geochim. Cosmochim. Acta* **60**, 415–422.
- Seyfried W. E. Jr., Janecky D. R., and Mottl M. J. (1984) Alteration of the oceanic crust: Implications for geochemical cycles of lithium and boron. *Geochim. Cosmochim. Acta* **48**, 557–569.
- Sisson T. W. and Grove T. L. (1993) Experimental investigations of the role of H_2O in calc-alkaline differentiation and subduction zone magmatism. *Contrib. Min. Petrol.* **113**, 143–166.
- Sisson T. L. and Layne G. D. (1993) H_2O in basalt and basaltic andesite glass inclusions from four subduction-related volcanoes. *Earth Planet. Sci. Lett.* **117**, 619–635.
- Stolper E. and McSween H. Y. Jr. (1979) Petrology and origin of the shergottite meteorites. *Geochim. Cosmochim. Acta* **43**, 1475–1498.
- Wadhwa M., McSween H. Y. Jr., and Crozaz G. (1994) Petrogenesis of shergottite meteorites inferred from minor and trace element micro-distributions. *Geochim. Cosmochim. Acta* **58**, 4213–4229.
- Wadhwa M. and Crozaz G. (1995) Trace and minor elements in minerals of nakhlites and Chassigny: Clues to their petrogenesis. *Geochim. Cosmochim. Acta* **59**, 3629–3645.
- Watson L. L., Hutcheon I. D., Epstein S., and Stolper E. M. (1994) Water on Mars: Clues from deuterium/hydrogen and water contents of hydrous phases in SNC meteorites. *Science* **265**, 86–90.
- Wilson L. and Head J. W. (1981) Ascent and eruption of basaltic magma on the Earth and Moon. *J. Geophys. Res.* **86**, 2971–3001.